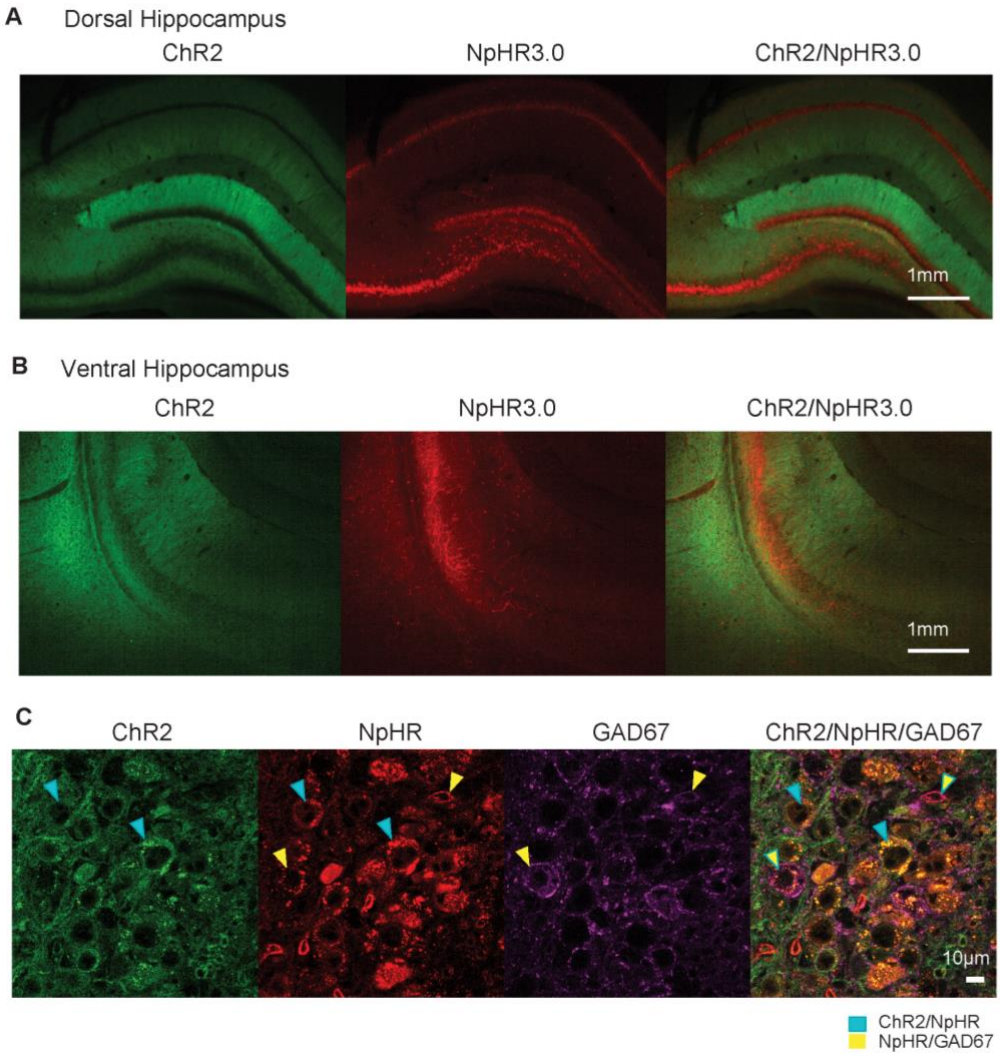

Supplementary Figure 1: Expression of CaMKII-ChR2-YFP and eNpHR3.0-mCherry in the dorsal and ventral hippocampus following co-injection of 2 separate viral vectors. (A) and (B) Widefield fluorescence images of the ipsilateral dorsal and ventral hippocampi respectively. (C) Confocal images within the ventral hippocampus show that expression of ChR2-YFP is localized in the soma and dendrites whereas eNPHR3.0 is predominantly localized in the soma. NpHR3.0-mCherry cells co-localize with CaMKII positive cells as well as CaMKII-negative cells. Blue arrows indicate colocalization of ChR2 and NpHR3.0, whereas yellow arrows indicate colocalization of NpHR3.0 with inhibitory GAD67-positive cells. NpHR3.0-positive cells that did not co-localize with ChR2-YFP positive cells tended to co-localize with inhibitory GAD67 positive cells.

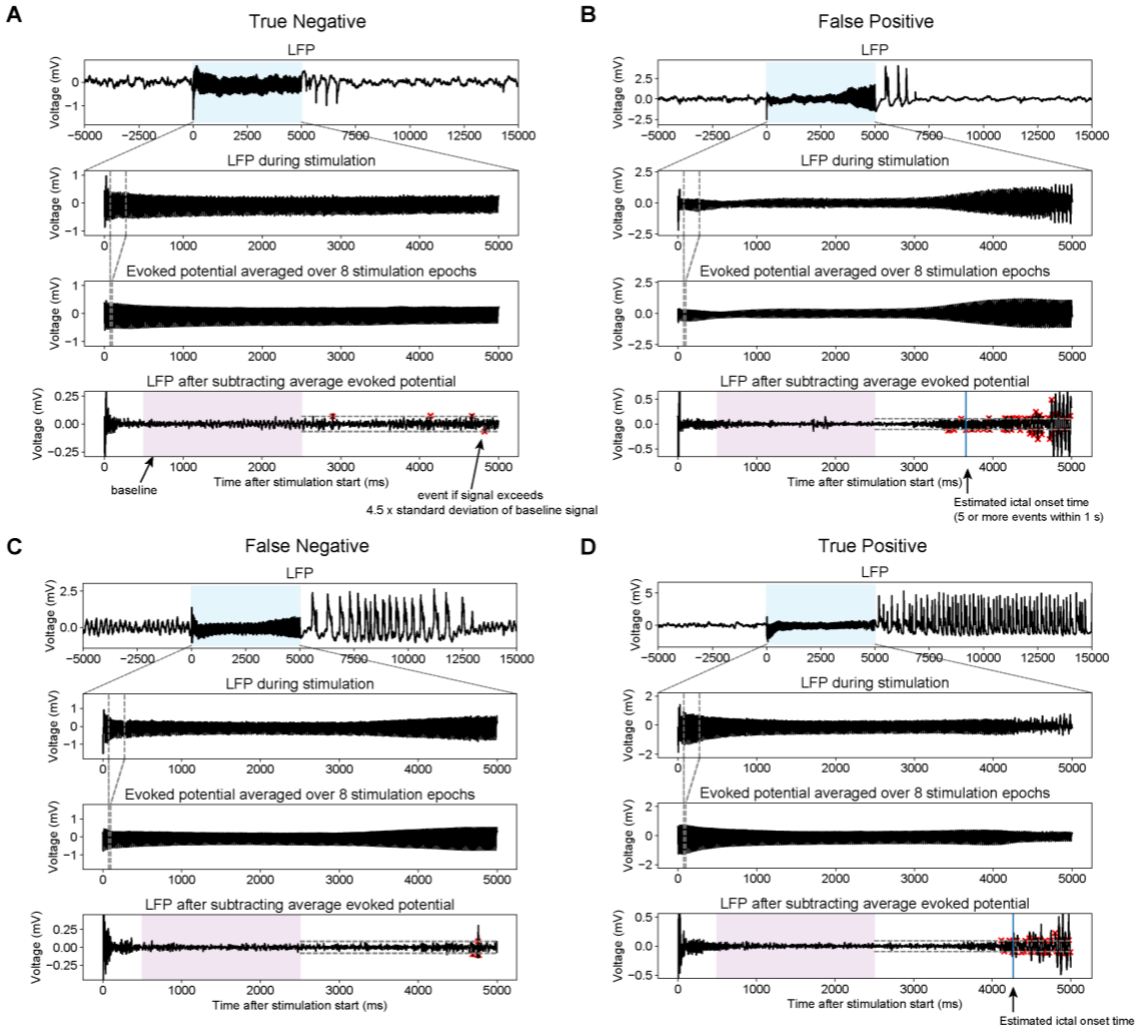

Supplementary Figure 2: Examples showing the procedure for estimation of onset time alongside correctly classified, false negative and false positive examples. Each example shows 4 rows which consist of (from top-to-bottom): (i) the raw LFP data, (ii) the LFP during the stimulation period after mean centering each epoch, (iii) the sliding-window mean evoked potential averaged over 8 epochs and (iv) the LFP after subtracting the sliding-window average evoked potential. The final row indicates the threshold for detection of spiking events (dashed-line) calculated as 4.5× the standard deviation of the baseline, where the baseline period is indicated by the shaded purple area and defined to be between 500-2500 ms from the stimulation onset. (A)-(D) Indicate examples of trials that were classified as true negative, false positive, false negative and true positive respectively.

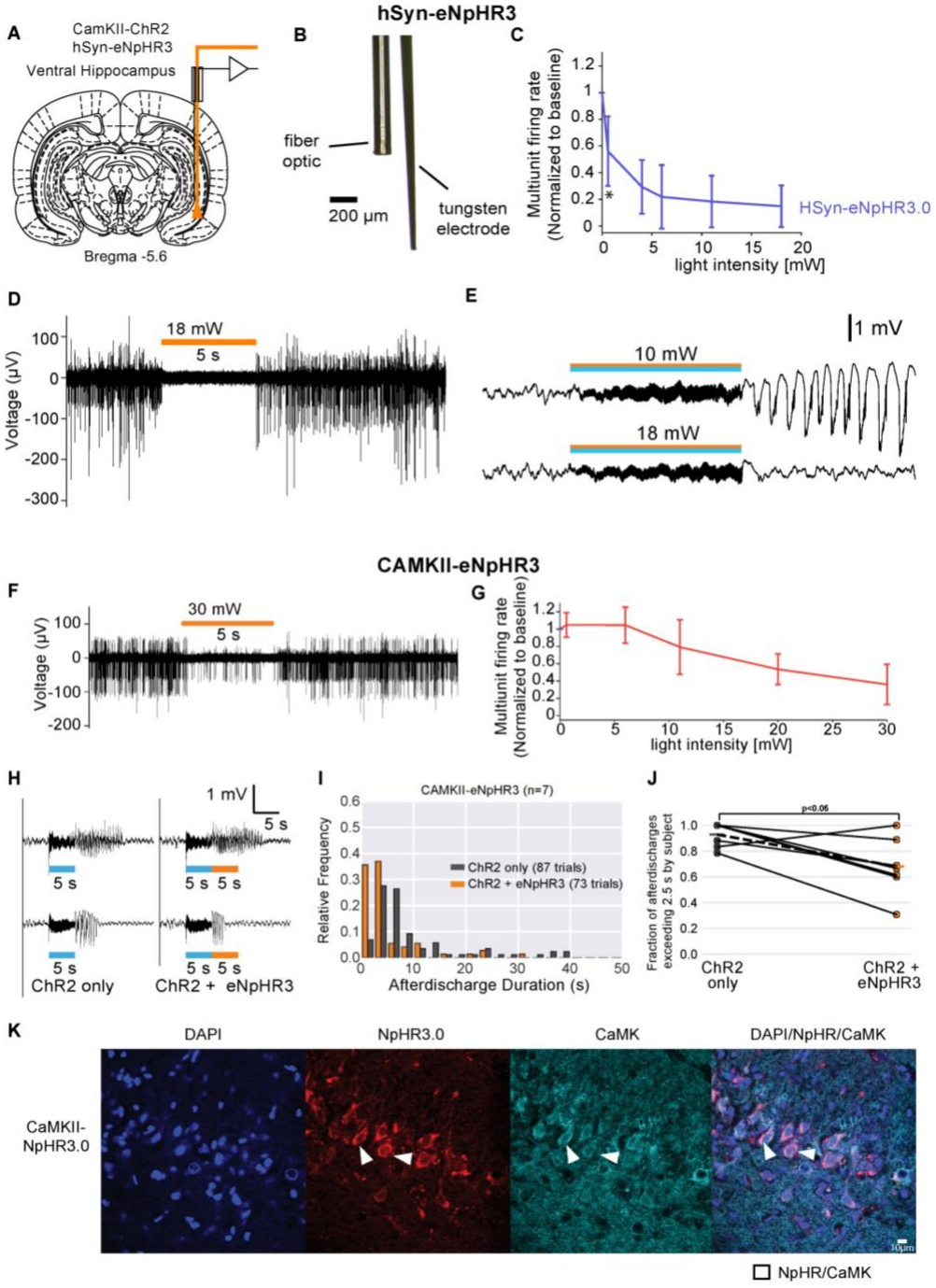

Supplementary Figure 3: hSyn-eNpHR3.0 optogenetic inhibition suppresses local spiking activity and prevents afterdischarges if applied simultaneously during optogenetic stimulation. CAMKII-eNpHR3.0 was not effective at inhibiting spontaneous firing and curtailing ADs. (A) Optrodes were implanted into the ventral hippocampus for electrophysiology and optogenetic excitation and inhibition. (B) Photograph taken under a light microscope of the tungsten optrode used for multiunit recordings. The tip of the electrode was measured to be approximately 0.65 mm from the fiber tip to ensure that the multiunit recording took place in the cone of illumination originating from the fiber tip. (C) Multiunit

firing rate during the stimulation period as a fraction of the baseline firing rate for hSyn-eNpHR3.0 expressing rats (n=2 animals, 21-30 trials for each light power) Data are plotted as the mean ± standard deviation across trials. (D) Example of a single trial multiunit recording trace from a rat expressing eNpHR3.0 under the hSyn promoter at the highest light power (18 mW) used during recordings. (E) Where ChR2 and eNpHR3.0 were stimulated simultaneously, higher light intensities were also more effective at preventing the onset of ADs. where the upper panel show example illustrating that lower light powers e.g. <10 mW may be insufficient to prevent the onset of afterdischarges when neurons were optogenetically excited and inhibited simultaneously. Lower panel indicates that during the same session, if the power is increased e.g. to 18 mW, then optogenetic inhibition prevented the occurrence of ADs. * indicates the mean firing rate is less than the baseline based on a one-sample t-test and a significance level of $p<0.05$. (F) Example of a single trial multiunit recording trace from a rat expressing eNpHR3.0 under the CAMKII promoter at the highest light power (30 mW). (G) Multiunit firing rate during the stimulation period as a fraction of the baseline firing rate for CAMKII rats (n=2 animals, 15-30 trials for each light power, except for 0.5, 6 and 20 mW which only include data from a single animal). Data are plotted as the mean ± SD across trials. (H) Example LFP traces from rats expressing CAMKII-eNpHR3.0 illustrating examples where optogenetic inhibition was considered to have failed to curtail ADs (top panels) and where optogenetic inhibition was considered to have succeeded in curtailing ADs (lower panels). The traces on the left and right panels are from the same recording sessions. The left panels are from stimulations consisting of the control condition (ChR2 only) and the right panels are from where the optogenetic inhibition has been applied immediately following the ChR2 blue light stimulation. (I) Histograms of AD duration for the two different stimulation conditions. (J) Proportion of ADs exceeding 2.5 in duration for the two different conditions. $p<0.05$ based on paired t-tests for n=7 subjects. (J) Confocal immunofluorescence from rats injected with CaMKII-eNpHR3.0-mCherry, CaMKII staining indicates NpHR-mCherry cells co-localize with CaMKII positive cells.

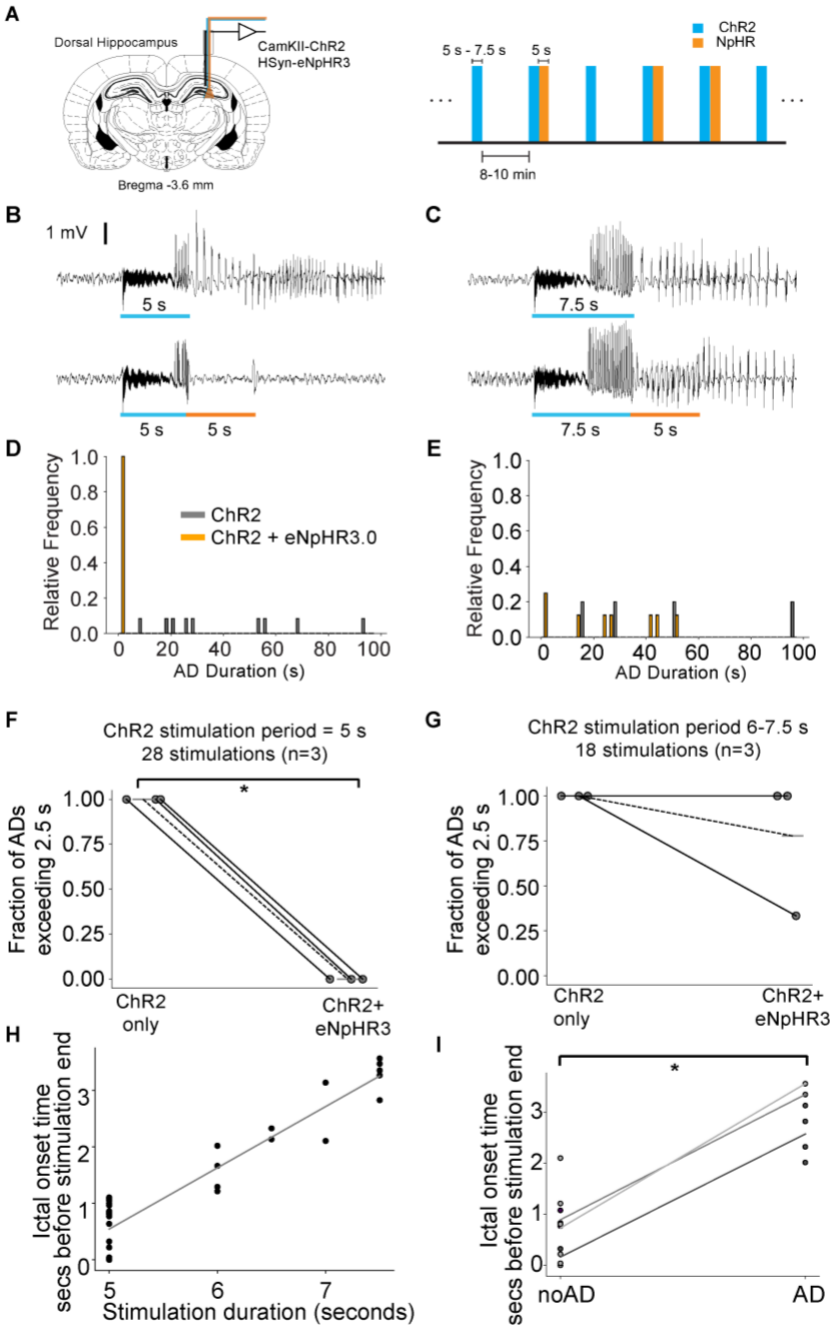

Supplementary Figure 4: Local optogenetic inhibition is able to curtail afterdischarges in the dorsal hippocampus for 5 s duration stimuli but not for longer duration stimuli. (A) Optrodes were implanted into the dorsal hippocampus for electrophysiology and optogenetic excitation and inhibition. (B) LFP traces from hSyn-eNpHR3.0 rats illustrating the generation of an AD from 5 sec stimulation without inhibition (upper) and a failed attempt at AD attenuation with optogenetic inhibition (lower). (C) Representative LFP traces from hSyn-eNpHR3.0 rats illustrating the generation of an AD from 6-7.5 s stimulation without inhibition (upper) and successful AD attenuation with optogenetic inhibition

(lower). (D) Histogram of AD duration for 5 seconds of stimulation only (blue) and stimulation with subsequent inhibition (orange). (E) Histogram of AD duration for 6-7.5 seconds of stimulation only (blue) and stimulation with subsequent inhibition (orange). (F) Proportion of ADs exceeding 2.5 s for ChR2 stimulations of 5 s in duration with and without inhibition. (G) Proportion of ADs exceeding 2.5 s for ChR2 stimulations of 6-7.5 s in duration with and without inhibition. (H) Estimated ictal onset time vs. stimulation duration. (I) Estimated ictal onset time vs. whether the AD exceeded 2.5 s.

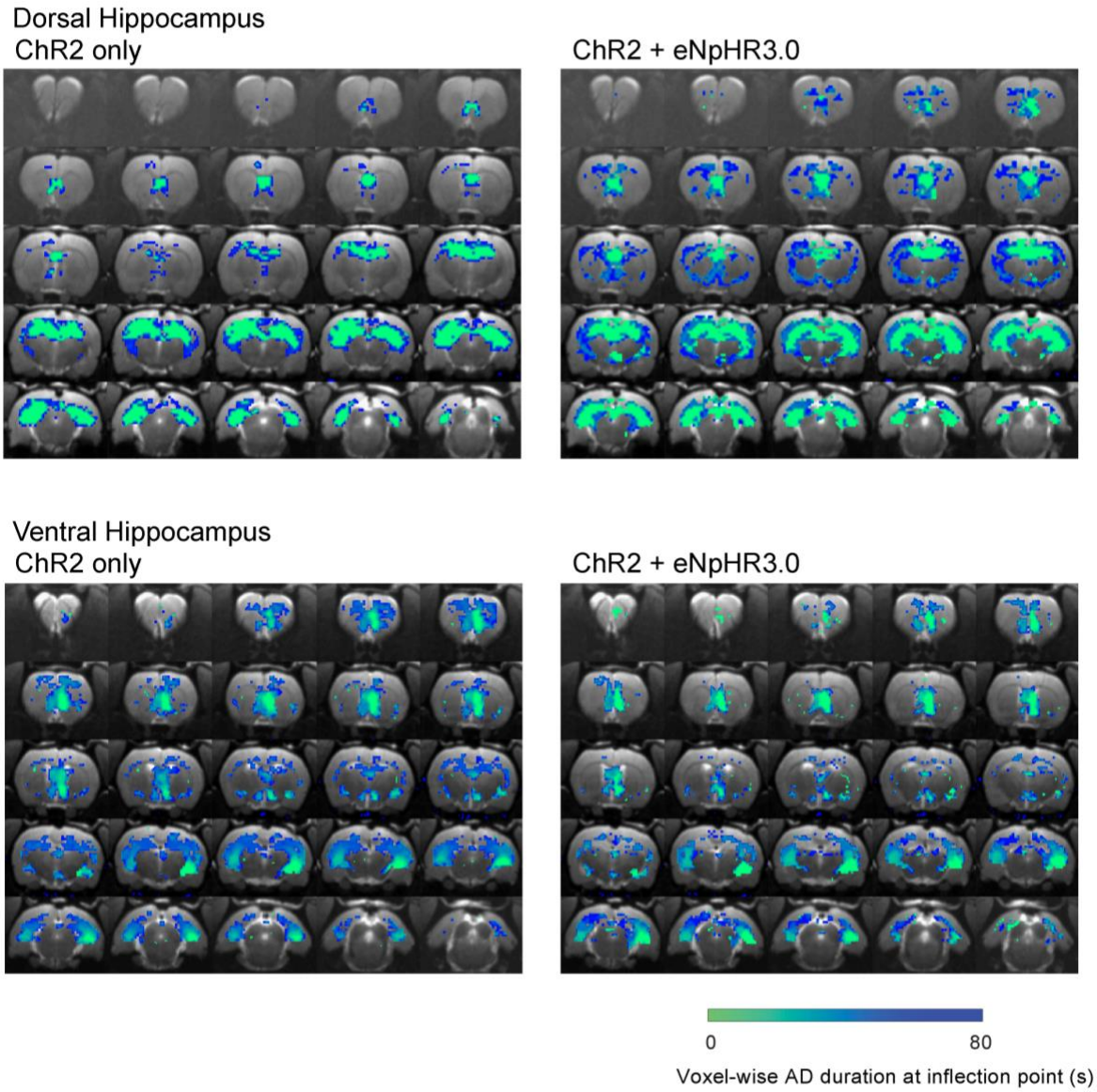

Supplementary Figure 5: Voxel-wise activation time maps with and without halorhodopsin inhibition. There were no obvious differences between the activation time maps with and without optogenetic inhibition from afterdischarges originating from either the dorsal or ventral hippocampi, therefore these data were combined for the analysis in **Fig. 4**.

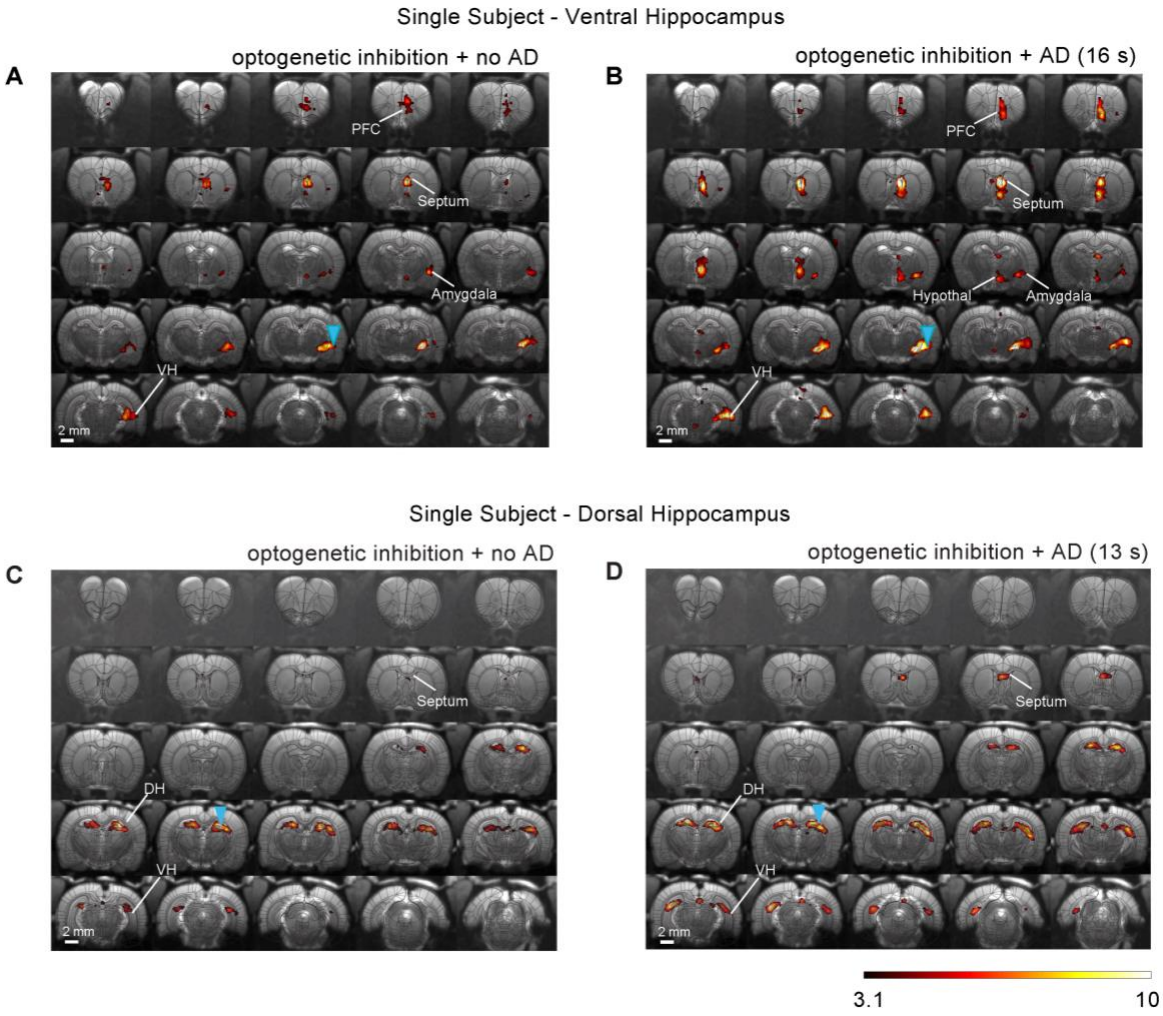

Supplementary Figure 6: Examples of optogenetic fMRI activation maps for individual trials in the ventral and dorsal hippocampus. Activation maps correspond to the same trials as the time series in Fig. 4c,d and Fig. 5c,d. Dorsal Hippocampus**:** (A) single-trial fMRI activation map (t-statistic) of short duration AD that was curtailed by optogenetic inhibition. (B) fMRI activation map of short duration AD that progressed despite optogenetic inhibition. Ventral Hippocampus: (C) fMRI activation map of short duration AD that did not progress to AD in the face of optogenetic inhibition. (D) single-trial fMRI activation map (t-statistic) of a short duration AD that was not curtailed by optogenetic inhibition. T-statistic maps are thresholded at $p<0.001$, uncorrected.

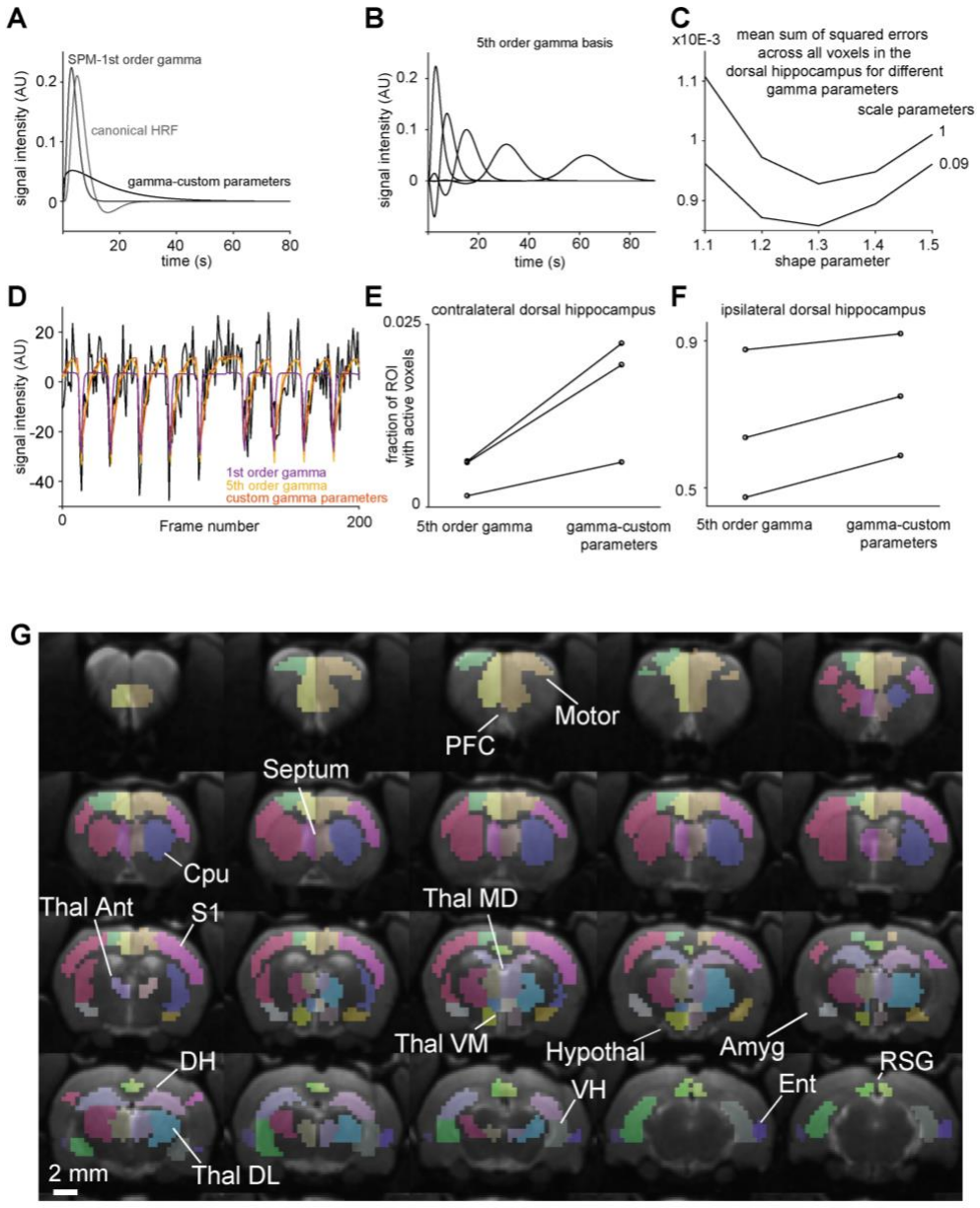

Supplementary Figure 7: CBV-weighted fMRI response to optogenetic stimulation in the dorsal hippocampus may be more appropriately described using a gamma distribution function with custom parameters compared to the canonical HRF or a more flexible 5th order gamma basis set as it has a faster onset and slower decay. (A) Example of gamma function with the best fitting parameters in comparison to the canonical HRF and SPM 1st order gamma. (B) 5th order gamma basis set. The higher order functions are able to account for significantly slower responses compared to the functions shown in *(A)*. (C) Mean sum of squared errors in the fit across all voxels in the ipsilateral dorsal hippocampus for different gamma shape and scale parameters, indicating the estimated optimal fit results from using shape and scale parameters of 1.3 and 0.09 respectively. (D) Example of fitted HRFs to block-design stimulation data. Here the measured and fitted responses are shown for 9 periods, where each period

consisted of a 5 s stimulation block at 40 Hz and 55 s rest block. The data were collected from least 3 six cycle acquisitions per subject in 3 subjects. Activation volumes expressed as a fraction of the total ROI volume in the contralateral (E) and ipsilateral (F) dorsal hippocampus respectively. Activation volumes are greater for the gamma-custom parameter model compared to the 5^{th} order gamma model as the single custom gamma function uses fewer parameters and is therefore more parsimonious. (G) Example segmentation used for the region-wise analysis of ofMRI data. All structural and functional images were aligned to a common subject space which was first segmented by registration to an atlas (Valdés-Hernández et al., 2011) and then manually corrected. Abbreviations: Amyg – Amygdala, Cpu – Caudate Putamen, DH – Dorsal Hippocampus, Ent – Entorhinal Cortex, Hypothal – Hypothalamus, PFC – Prefrontal Cortex, RSG – Retrosplenial Cortex, S1 – Primary Somatosensory Cortex, Thal Ant – Anterior thalamus. Thal DL – Thalamus Dorsal Lateral, Thal MD – Thalamus Medial Dorsal, Thal VM – Thalamus Ventral Medial, VH – Ventral Hippocampus.